

Dielectric Constant of Sintered Compact of Oriented Barium Titanate Short Fibers Doped with Mica

(the Late) Young-Jin Park,# Kaoru Igarashi,* and Tadao Shimizu

Department of Industrial Chemistry, Chiba Institute of Technology, 2-17-1 Tsudanuma, Narashino-shi, Chiba 275-0016

(Received November 20, 2000)

A compact consisting of $BaTiO_4$ fibers oriented mostly in one direction was fabricated via piling sheets made by the doctor blade method. After calcination, in the obtained sintered-compact, the shape of individual fibers was 1ost and spherical ceramic grains appeared. Nevertheless the *c*-axis of micro-crystals of the ceramic was oriented mainly in the direction of the press that had been applied to the green compact in the fabrication process. Although the compacts were calcined at 1250 °C, which is 1ower than the calcination temperature of typical $BaTiO_3$, the densities of the obtained sintered compacts were high because of the addition of mica. The relative dielectric constant of the 2% doped sample was higher by 1000 than that of the undoped matelia1. $BaTiO_3$ doped with mica by 5% had a dielectric constant independent of frequency in the range of 100 Hz to l MHz.

Because particles of $BaTiO_3$ powder ordinarily take a spherical form, the crystal axes in the grains in sintered compacts lie in random direction, and no anisotropy is observed throughout the entire sintered compact. Studies[1–5] on the alignment of plate-like grains of bismuth titanate sintered compacts have been performed. The degree of orientation of crystal axes was also estimated via powder X-ray diffraction.[6] Ohara, et a1.[7–8] succeeded in producing an anisotropical $BaTiO_3$ piezoelectric ceramic from a green compact whose fibrous particles were oriented by compressing in two directions.

In this study, we attempted to produce anisotropical dielectrics without app1ying electrical poling from $BaTiO_3$ short fibers.[9] In the process, raw material powder was doped by synthetic mica, whose particles were micro-thin plates because of cleavage. Mica is expected to contribute to aligning fibrous particles and 1owering sintering temperature, due to its particle shape and 1ow melting point.

Experimental

Raw Materials. Hydrated titanium dioxide short fiber ($TiO_2 \cdot 2H_2O$), barium hydroxide ($Ba(OH)_2 \cdot 8H_2O$, reagent grade, Kishida Chemicals) and synthetic mica (Kopu Chemica1) were employed. The composition of synthetic mica was Si: 26.7, Mg: 16.5, F: 3.6 and K: 6.2 (mo1%) particles, and the melting point was l220 °C. Fig. 1(a) is a scanning electron micrograph of plate-like synthetic mica particles approximately l0 μm in diameter.

Synthesis of $BaTiO_3$ Short Fibers We synthesized hydrated TiO_2 short fibers using the ion-exchange method that was shown in our previous paper.[9] The hydrated titanium dioxide fiber (Fig. 1(b)) and barium hydroxide were mixed in equal mole percent amounts. This mixture was subjected to a hydrothermal process for 48 h at 160 °C in an autoclave. The resultant product was separated by filtration, washed repeatedly with deionized water, and then dried for 24 h at 30 °C. The $BaTiO_3$ fiber shown in Fig. 1(c) was obtained and identified via powder X-ray diffraction. The diameter and the length of the fiber ranged 1–3 μm and 30–60 μm, respectively.

Compact Pressed in One Direction. $BaTiO_3$ fibers were dispersed in water and deposited on a paper filter in a Buechner funne1. The deposit was dried and pressed in the direction of the deposition (Fig. 2(A)). $BaTiO_3$ fiber packed in a mold was pressed in one direction for l min at 27 MPa. The sample obtained was 2 mm thick. After drying, the pressed compact was calcined at l000–1350 °C in an electric furnace.

Compact of Fibers Oriented in One Direction. Figure 2(B) shows the experimental procedure. $BaTiO_3$ fiber added with 0–5 mass% of synthetic mica is mixed with a dispersion medium containing toluene 98 vol%, polyethylene glyco1 1 vo1% and l mass%-polyvinylalcohol aq. solution l vo1%. The mixture is stirred using a magnetic stirrer to obtain slurry. It was then poured into a box with a blade attached (Fig. 2(a)). The box was moved in a direction so as to spread the slurry to be a thick film by limiting the thickness with the blade; this is called the doctor blade method,[10–12] developed for tape casting. The sheet, whose thickness ranges from approximately 500 to 1000 μm, becomes l00–200-μm thick after drying in air. The dried sheets are stacked 50–100 times, pressed for l min with an iron at 200 °C and further in a mould by 27 MPa, and then calcined at 1000 °C for l h. The obtained compact is like a piece of dice with the dimension of about 10 mm. It was cut in two directions into 2-mm thick plates as shown in Fig. 2(d) and (e). The plates were sintered at 1250 °C.

Measurement. To the sample plate (d) and (e) in Fig. 2, voltage application for dielectric constant measurement, X-ray irradiation for XRD, and SEM observation were performed in the directions parallel (||) and vertica1 (⊥), respectively, to the pressed directions for step (c).

Particle orientation in the sintered compacts was identified using X-ray powder diffraction (RINT-l500, Rigaku Denki) and particle morpho1ogy by scanning electron microscopy (SEM) (TL200, Nippon Electronics). Both sides of the compact were thin1y coated with silver paste, dried and heated for 10 min at 500

Deceased in December 2, 2001.

°C in an electric furnace. Dielectric constant and dielectric loss were measured using a LCR meter (4192A, Yokogawa Hewlett-Packard) operating at an alternating voltage.

Results and Discussion

Compact Pressed in One Direction. In the green compact of Fig. 2(A), due to the press of the deposition of fiber, a large ratio of fibers is presumed to lie parallel to the bottom plane, but the direction is random.

The raw materia1, hydrated titanium dioxide short fiber was obtained from $K_2Ti_4O_9$ fiber with an ion exchange process. The $K_2Ti_4O_9$ fiber supposed to be single crysta1, because $K_2Ti_6O_{13}$ fiber synthesized via the same method was recognized to be single crysta1.[13] The $BaTiO_3$ fiber is obtained after two ion exchange processes. As even the crystal structure changes in the second process, the fiber may not be single crystal. We discuss the $BaTiO_3$ fiber as polycrystalline below.

Table l shows the intensity ratio of X-ray diffraction of cubic $BaTiO_3$. Concerning the difference from (||)′ surface, there is no particular difference from the JCPDS card.[14] If the a-axis of the crystal lies in the direction of the radius of the fiber, diffraction from (001) plane would be stronger than diffraction from others. The column (⊥)′ shows the intensity ratio of X-ray diffraction patterns of the surface that was vertical to the pressed direction and includes information about cut surfaces of fibers. The intensity of (112) plane is much larger than that

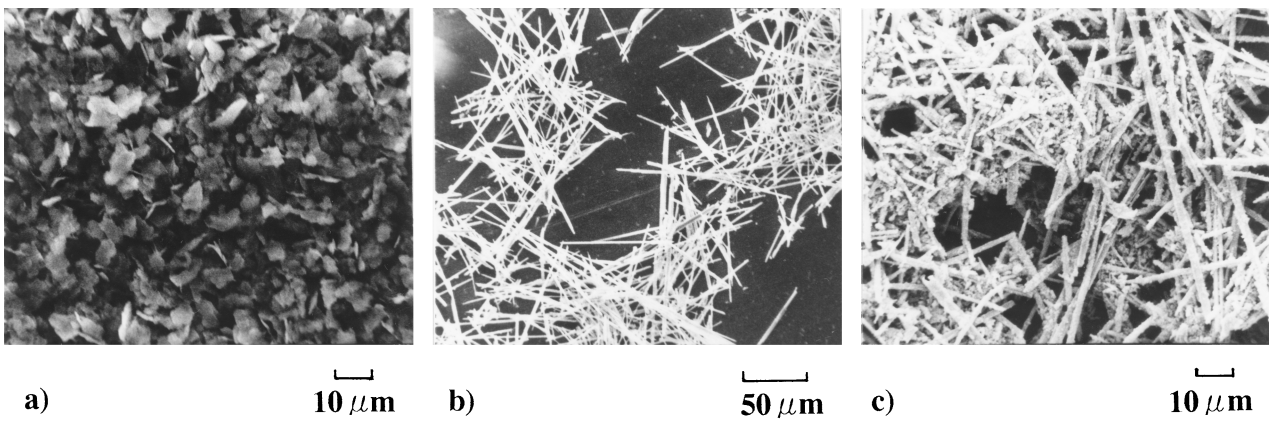

Fig. 1. Scanning electron micrographs of the reactants. (a) Synthetic mica, (b) Hydrated titanium dioxide fiders, (c) $BaTiO_3$ fibers.

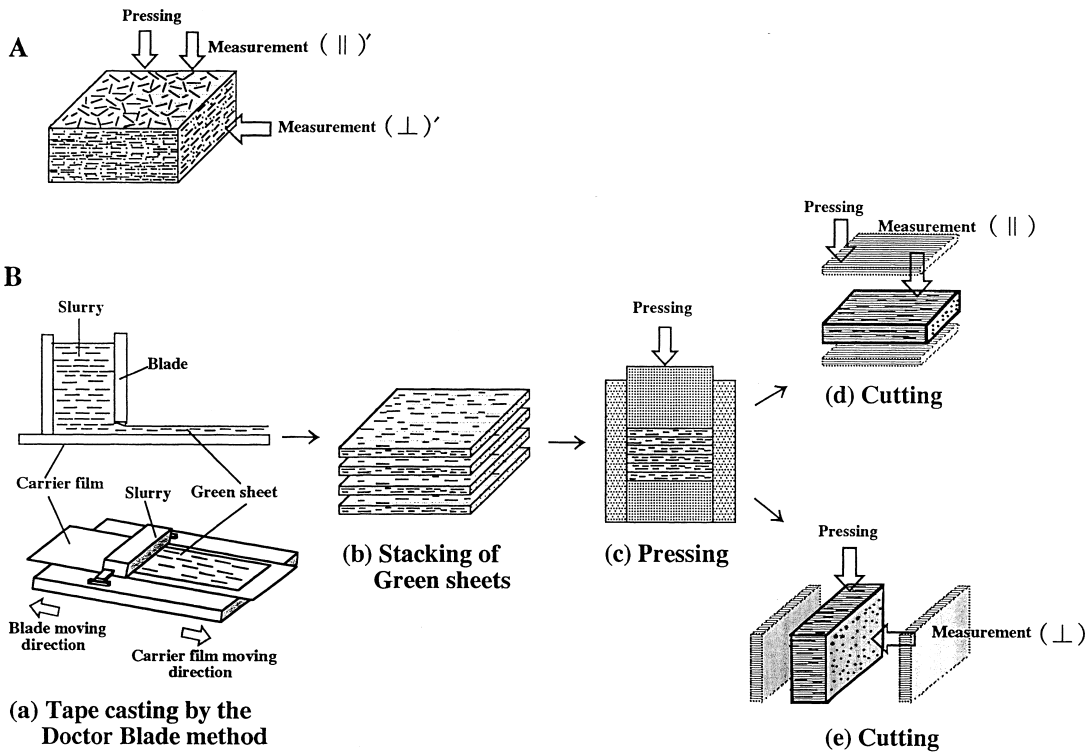

Fig. 2. (A) Compact pressed in one direction after deposition in a Buefner funnel. (B) Process of fabrication of compact of fibers oriented in one direction, and cutting after calcination.

Table 1. Intensity Ratio of X-ray Diffraction of Cubic $BaTiO_3$ for Comparison of Non-Oriented Powder (JCPDS) and Non-Calcined Compact Pressed in One Direction

JCPDS No. 31-174[14]				(‖)′	(⊥)′
2θ	d(Å)	hk1	I/I°	I/I°	I/I°
22.0	40.4	001	14	19	26
31.4	2.85	101	100	100	100
38.7	2.32	111	30	20	23
44.9	2.01	002	35	27	40
50.6	1.80	102	10	8	16
55.9	1.64	112	25	23	81
65.5	1.42	202	15	17	50

(‖)′: The measured surface was parallel to the press direction. (⊥)′: The measured surface was vertical to the press direction. *I*/*I*°: Intensity ratio of diffraction comparing to the maximum .*d*: Spacing. θ: Bragg angle with regard to Cu $K\alpha_1$.

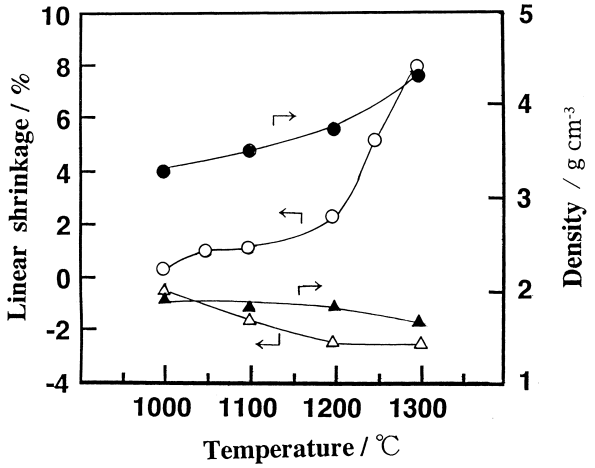

Fig. 3. Linear shrinkage and density of the compact made of each component powder vs. calcination temperature.
○●: $BaTiO_3$fiber △▲: Synthetic mica.

on the JCPDS card. These results indicate that the crystal axes do not lie in the direction of the length or the cross-section of the fibers.

Figure 3 shows density and linear shrinkage at various calcination temperatures of compacts of $BaTiO_3$ fiber of Fig. 2(A) and of synthetic mica pressed in one direction. A mild linear shrinkage of 0–2% was exhibited at 1000–1200 °C, while there were increases at temperatures above l200 °C. The density of the compact calcined at l300 °C was 4.2 g/cm^2, which is a relative density of 72% compared to $BaTiO_3$ single crystal.

Figure 4 shows the relationship between frequency of applied voltage and dielectric constant of sintered compacts calcined at various temperatures. The dielectric constant increased as the calcination temperature increased. This corresponds to an increase in relative density. The dielectric constant of the sample calcined at 1350 °C is close to that of typical $BaTiO_3$. Concerning samples calcined at 1250 °C or 1ower temperatures, the dielectric constant was high only at 1ow frequencies. This is thought to reflect insufficient particle growth and high porosity. This dielectric constant is an apparent one

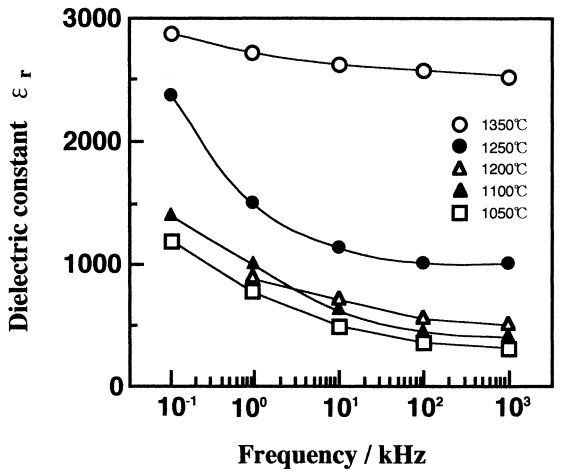

Fig. 4. Dielectric constant of compacts of $BaTiO_3$ fiber calcined at different temperature.

due to the surface electrical charges between grain particles, not due to dense matter.

Figure 5 shows X-ray diffraction patterns of sintered compacts of oriented fibers of $BaTiO_3$ with and without synthetic mica. The sintered compact doped with 5% mica contains by-products, while the others show almost the same pattern as $BaTiO_3$. The separation of peaks of (200) and (002) planes of tetragonal system is not clear because of the 1ow resolution of the measurement.

Compacts of Fibers Oriented in One Direction. Figure 6(a) is the scanning electron micrograph of a pressed surface of a green compact of $BaTiO_3$ fibers which are oriented parallel to each other. Figure 6(b) shows the compact calcined at 1250 °C. It appears to consist of spherical particles and the shape of fiber is lost.

Figure 7 is the X-ray diffraction pattern around $2\theta = 45°$ for the sample doped with mica by 2%. The peak at 44.8° is assigned to the (002) plane, while that at 45.1° is assigned to the (200) plane.[15] In Fig. 7(a) the peak of the sample (‖) assigned to the (002) plane is larger than that assigned to (200), i.e. $I_{002} > I_{200}$, which is contrary to typical $BaTiO_3$ ceramics. This means that a large ratio of micro-crystals orient with their *c*-axis para11el to the direction of the thickness. This is an anisotropical orientation. On the other hand, in Fig. 7(b) the sample (⊥) exhibits $I_{002} < I_{200}$. This is almost the same as for normal $BaTiO_3$ ceramic. The presence of the (002) peak means that the degree of anisotropical orientation is not very high. During sintering, the system is thought to be cubic because the temperature is over the phase transition temperature, i.e. the ferroelectric Curie temperature, 120 °C for pure $BaTiO_3$.[16] Therefore, the obtained anisotropy that was illustrated with the distribution of *c*-axes must have appeared at room temperature after sintering.

Figure 8(a) illustrates the model of the orientation of micro-crystals in the $BaTiO_3$ short fiber, in which *a*-axes of micro-crystals in cubic system are parallel to each other in each part. Figure 8(b) shows spherical grains that appeared after sintering and micro-crystals in the grains. The crystal is cubic at sintering temperatures, and changes into tetragonal when the temperature drops to room temperature. Every axis seems equiva-

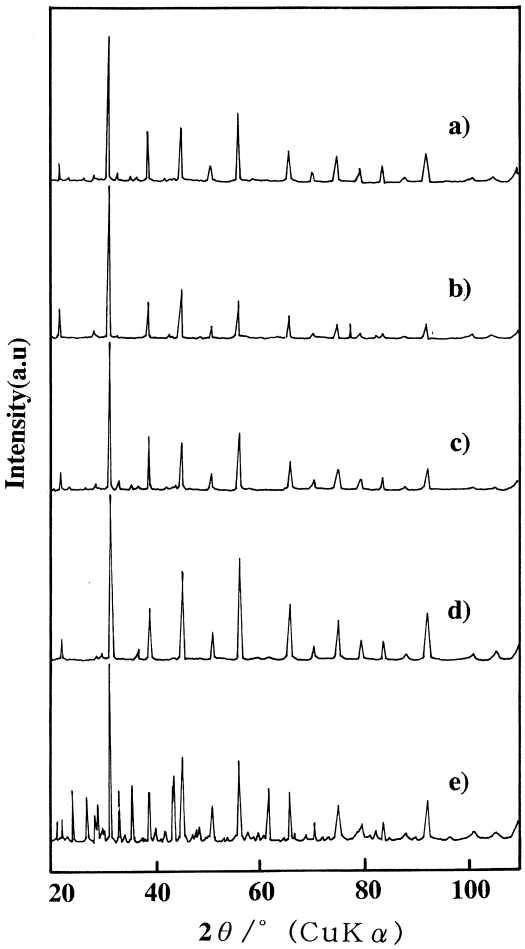

Fig. 5. X-ray powder diffraction patterns of $BaTiO_3$ compacts (||)′ after calcination at 1250 °C. Synthetic mica was added by (a) 0%, (b) 1%, (c) 2%, (d) 3%, and (e) 5%. θ is regarding to Cu $K\alpha_1$.

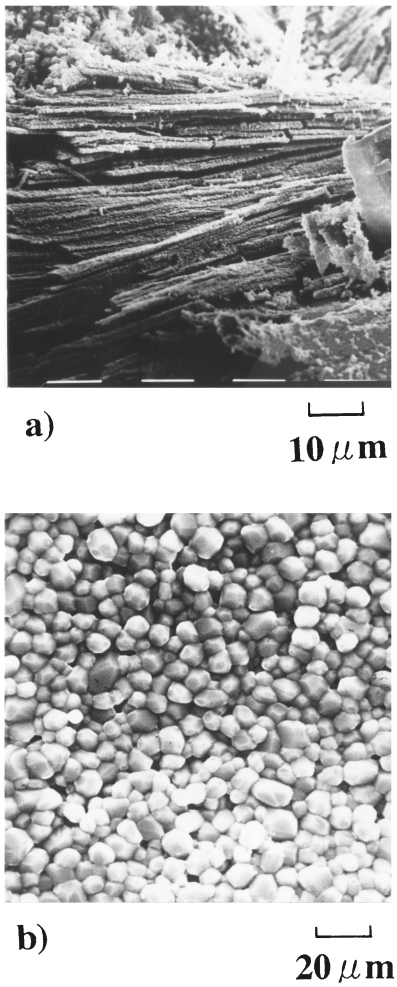

Fig. 6. Scanning electron micrographs of (a) the green $BaTiO_3$ fiber compact and (b) the calcined compact observed in the direction (⊥) to the sample surface.

lent, but *c*-axis appeared to be in a particular direction. Here, we call this situation anisotropica1 orientation of micro-crystal. The cause is not clear, but may be ascribed to some distribution of density in the compact.

Figure 9 shows the linear shrinkage of the thickness of the sample plates (||) and (⊥) during sintering at 1250 °C for l h. The shrinkage of the (⊥) sample remained almost constant regardless of the amount of mica added. From such a result it seems that the fiber itself does not shrink. On the other hand, in the (||) sample, linear shrinkage increased from 2% to 10% with the amount of mica added. In the (||) sample, the space among fibers and plate-like mica decreases during sintering.

Dielectric Characteristics of Sintered Compacts. Figure l0 shows the dielectric constant measured at l MHz of sintered compacts which were made at 1250 °C from fibrous $BaTiO_3$ and synthetic mica. (⊥) samples doped with synthetic mica by 2% exhibited the highest dielectric constant. The relative dielectric constant of (⊥) samples was higher by 1000 than that of the undoped one. Presumably the ferroelectric Curie temperature of the 2% sample is close to room temperature, because most additives lower the Curie temperature of $BaTiO_3$ and the dielectric constant becomes a maximum at that temper-

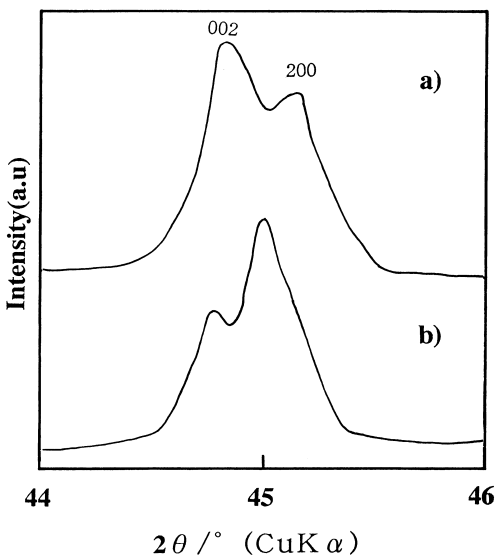

Fig. 7. X-ray powder diffraction patterns of $BaTiO_3$ compact calcined at 1250 °C: (a) (||) plane, (b) (⊥) plane. θ is regarding to Cu $K\alpha_1$.

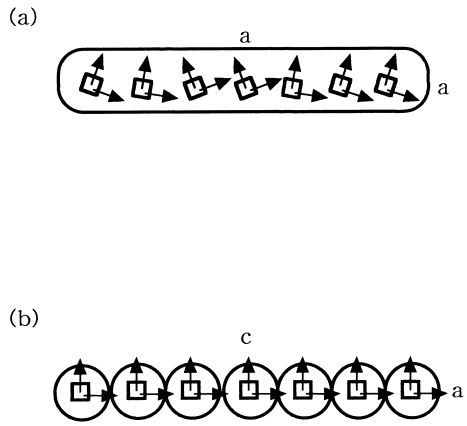

Fig. 8. Model of the orientation of micro-crystal axes in (a) $BaTiO_3$ short fiber and (b) grains after sintering.

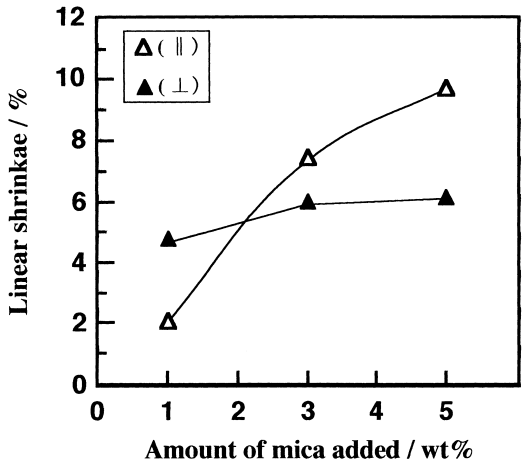

Fig. 9. Linear shrinkage samples (∥) and (⊥) calcined at 1250 °C in the direction of thickness.

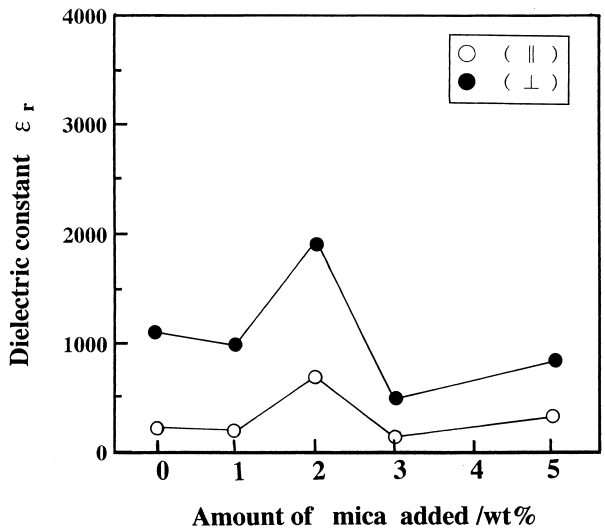

Fig. 10. Dielectric constant of $BaTiO_3$ fiber measured at 1 MHz as a function the amount of doped mica.

ature. (⊥) samples exhibit larger dielectric constant than (∥) samples. Generally, $BaTiO_3$ single crystal has a larger dielectric constant in the direction of *a*-axis than *c*-axis.[17] The result indicates that micro-crystals with the *a*-axis para11el to the direction of the electric field used in the measurement exist in high percentage. This corresponds to Fig. 7. The values of the non-doped sample are small comparing to those of typical $BaTiO_3$ ceramics, ~3000. This is because the raw material $BaTiO_3$ fiber contains impurities, mainly potassium ion, which were not removed perfectly during the preparation process. The influence is seen in Fig. 5(a) as X-ray peaks of biproducts.

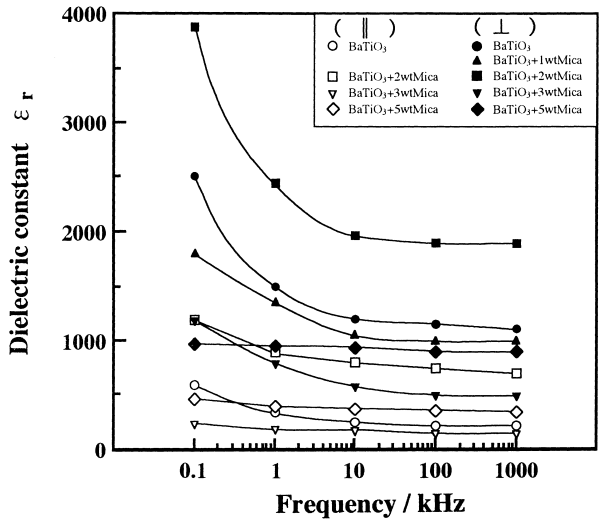

Fig. 11. Dielectric constant as a function of frequency of applied electric field.

Figure 11 shows the relationship between the relative dielectric constant and the frequency at which the measurement is conducted. The dielectric constant of samples doped be1ow 3% exhibit an increase as the frequency decreased. This is thought to be ascribed to insufficiency of sintering and porosity as described in Fig. 4. The dielectric constant of a sample doped with 5% mica remained unchanged from 100 Hz to l MHz. This means that the influence of the surface electrical charge of grains did not appear even at low frequencies. This corresponds to the fact that this sample has a 1ow porosity, as shown in Fig. 9.

Figure 12 shows the 1oss tangent of the compacts of $BaTiO_3$ short fibers with and without synthetic mica which were sintered at 1250 °C. The dielectric loss was small for each composition at l MHz, while it was higher at l00 Hz. The sample doped with 5% mica exhibited a small dielectric loss and was scarcely influenced by the frequency. This corresponds to the results in Fig. 11, which showed the lack of influence of frequencies on the dielectric constant of samples containing 5% mica.

Conclusion

We produced two kinds of sintered compacts from pressed compacts of $BaTiO_3$ fibers to which synthetic mica was added. In green compact, fibers lie parallel to a plane, and fibers orient in one direction. Their dielectric properties were measured. The following results are obtained.

1. The orientation of short fibers in a green sheet made with the doctor blade method was observed using SEM. In the sin-

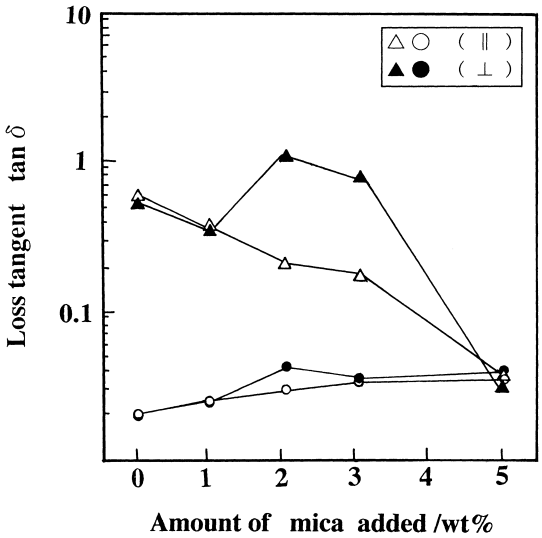

Fig. 12. Loss tangent as a function of the amount of mica added to $BaTiO_3$ fiber. △▲: the electric field at 100 Hz, ○●: 1 MHz.

tered samples, no shape of fibers was seen and spherical particles appeared. However, the dielectric constants differed depending on the original fiber orientation.

2. At the calcination temperature of 1250 °C, the relative dielectric constant of samples made from $BaTiO_3$ short fibers doped with synthetic mica by 2% was higher by 1000 than that of the sample without mica.

3. $BaTiO_3$ short fibers doped with 5% mica became a dielectric material independent of the frequency of electric field in the range of 100 Hz to l MHz.

4. Crystal axes did not tie in the direction of the length or the radius of raw material $BaTiO_3$ fiber before calcinations.

References

1 S. H. Lin, S. L. Swartz, W. A. Schulze, and J. V. Biggers, *J. Am. Ceram. Soc.*, **66**, 881 (1983).

2 Y. Nakamura, H. Igarashi, T. Taniai, and K. Okazaki, *Am. Ceram. Soc. Bull.*, **58**, 853 (1979).

3 Z. T. Zhang, K. Koumoto, and H. Yanagida, *Yogyo Kyokaishi*, **90**, 709 (1982).

4 H. Watanabe, T. Kimuma, and T. Yamaguchi, *J. Am. Ceram. Soc.*, **74**, 139 (1991).

5 S. Ikegami, and I. Ueda, *Jpn. J. Appl. Phys.*, **13**, 1572 (1974).

6 H. Tateyama, *Yogyo Kyokaishi*, **95**, 875 (1987).

7 Y. Ohara, K. Koumoto, and H. Yanagida, *J. Am. Ceram. Soc.*, **68**, c-108 (1985).

8 Y. Ohara, K. Koumoto, and H. Yanagida, *J. Am. Ceram. Soc.*, **77**, 2327 (1994).

9 T. Shimizu, H. Yanagida, M. Hori, K. Hashimoto, and Y. Nishikawa, *Yogyo Kyokaishi*, **87**, 500 (1979).

10 W. Class, *Research/Development*, March, 37 (1971).

11 K. Murakawa, *Ceramics Japan*, **12**, 207 (1977).

12 K. Niwa, *Ceramics Japan*, **19**, 146 (1984).

13 T. Shimizu, T. Morita, H. Yanagida, and K. Hashimoto, *Yogyo Kyokaishi*, **85**, 190 (1977).

14 S. Naka, F. Nakakita, Y. Suwa, and M. Inagaki, *Bull. Chem. Soc. Jpn.*, **47**, 1168 (1974).

15 JCPDS 5-626, JCPDS International Centre for Diffraction Data.

16 B. Jaffe, W. R. Cook, and H. Jaffe, "Piezoelecthc Ceramics," Academic Press (1971), pp. 53–107.

17 D. Berlincort and H. Jaffe, *Phys. Rev.*, **111**, 143 (1958).